Resonancelike responses of autonomous nonlinear systems to white noise

T. Ditzinger, C. Z. Ning,* and G. Hu†
Institut für Theoretische Physik und Synergetik, Universität Stuttgart, Pfaffenwaldring 57/IV, D-70550 Stuttgart, Federal Republic of Germany
(Received 5 January 1994; revised manuscript received 19 May 1994)

Responses of two models of autonomous nonlinear systems, one bistable and the other monostable in certain parameter regions, to additive white noise are investigated numerically. We show that the additive white noise can induce coherent oscillations, and both autonomous systems show optimum responses, represented by the maximum signal-to-noise ratio of the output for certain noise strengths. This phenomenon is thus termed as stochastic resonance without external periodic force.

PACS number(s): 05.40.+j, 05.20.−y

I. INTRODUCTION

The interplay among nonlinearity (usually bistability), periodicity, and randomness displays certain very interesting phenomena and has attracted the interest of many researchers recently. A recent example is the so-called stochastic resonance (SR) [1–11]. Here the three important ingredients, namely, bistability of the deterministic system, periodic modulation through an external signal, and randomness through stochastic force, join together and induce an enhancement in the signal-to-noise ratio (SNR) through their interplay. Natural extensions or variations of this study are to reduce some ingredients, or replace one or two of the three ingredients by some other similar mechanism. In this aspect, some examples have already been considered by a number of scientists: Benzi and co-workers [1] substituted noise by the deterministic stochasticity displayed by the Lorenz model; Stocks, Stein, and McClintock [12] replaced the bistable system by a monostable one; and we considered the SR-like phenomenon in autonomous bistable systems without adding a periodic signal [13].

In this paper we will further develop the idea in [13] and make a detailed investigation of SR without periodic force. In Sec. II we present two models of Langevin equations. The deterministic part of model 1 shows bistability while that of model 2 shows monostable behavior in certain parameter regions. In both models the systems are subjected to white noise but not to a periodic force. Since the models are too complicated for an explicit analytical solution, numerical simulation is used to study the system dynamics. In Sec. III we present and analyze the numerical results. There we will see how noise plays an active constructive role in stimulating coherent oscillations and how the noise-induced oscillation displays a resonancelike behavior so-called SR without periodic forcing. This SR exists for both bistable and monostable autonomous nonlinear systems.

*Permanent address: Arizona Center for Mathematical Sciences, University of Arizona, Tucson, Arizona 85721.

†Permanent address: Department of Physics, Peking Normal University, Peking 100875, China.

II. MODELS AND SIMULATIONS

Both models consist of a set of two Langevin equations,

$$dx = f_1(x,y)dt + dw_1 , \tag{1}$$

$$dy = f_2(x,y)dt + dw_2 , \tag{2}$$

where dw_1 and dw_2 are the uncorrelated Wiener process with the following moments:

$$\langle w_i \rangle = 0 , \tag{3}$$

$$\langle dw_i dw_j \rangle = dt\, D_i \delta_{ij}, \quad i,j = 1,2 . \tag{4}$$

For simplicity, we choose $D = D_1 = D_2$. For the deterministic drift forces we focus on two models.

A. Model 1

$$f_1(x,y) = x(1-x^2-y^2) + y(x^2-y^2-b) , \tag{5}$$

$$f_2(x,y) = y(1-x^2-y^2) - x(x^2-y^2-b) . \tag{6}$$

This model was analyzed in Ref. [14]. If we ignore the noise, the two deterministic equations can be rewritten in the form

$$\begin{aligned} \dot{r} &= r(1-r^2) , \\ \dot{\phi} &= b - r^2 \cos 2\phi , \end{aligned} \tag{7}$$

where we alternatively use a complex variable $u = r\exp(i\phi)$ or the corresponding polar coordinates r,ϕ. They are related to the old coordinates by $x + iy = r\exp(i\phi)$. The system has one unstable solution at the origin (0,0). Considering the asymptotic dynamics around the circle $r = 1$, one can find three different types of trajectories.

1. $b > 1$

A limit cycle on the circle $r = 1$ exists, denoted by I in Fig. 1(a).

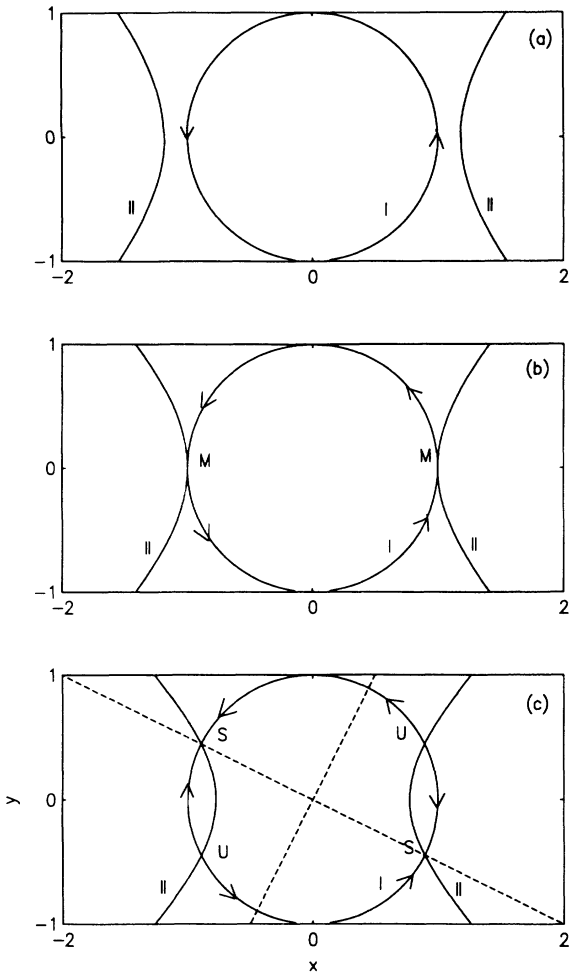

FIG. 1. Deterministic behavior of model 1. (a) $b > 1$, the case of the limit cycle. (b) $b = 1$, two fixed points M with marginal stability. Two heteroclinic orbits exist as indicated by the arrows. (c) $b < 1$, two stable fixed points S and two unstable fixed points U on the circle $r = 1$. The location of the fixed points is given by the intersections of the circle I ($r = 1$) and the curves II, defined by $b = x^2 - y^2$.

2. $b = 1$

As b decreases from $b > 1$, the period T of the limit cycle increases monotonically; in the limit $b \to 1$ we have $T \to \infty$. The limit cycle of the system vanishes at $b = 1$, and two fixed points with marginal stability appear via a saddle-node bifurcation, denoted by M in Fig. 1(b). The two arcs and the two stationary solutions on the circle $r = 1$ in Fig. 1(b) form two heteroclinic orbits, the upper one and the lower one.

3. $b < 1$

The two fixed points in Fig. 1(b) separate to two pairs of stationary solutions, which are given by

$$r = 1, \quad b = \cos 2\phi \ , \tag{8}$$

as can be seen in Fig. 1(c). In each pair one solution is stable and the other unstable, denoted in Fig. 1(c) by S and U, respectively. At this parameter value the system shows a typical bistability.

B. Model 2

$$f_1(x,y) = x(1 - x^2 - y^2) + y(x - b) \ , \tag{9}$$

$$f_2(x,y) = y(1 - x^2 - y^2) - x(x - b) \ . \tag{10}$$

This can be written in the polar coordinate system as

$$\dot{r} = r(1 - r^2) \ , \qquad \dot{\phi} = b - r\cos\phi \ . \tag{11}$$

For model 2 there exist three different cases, too.

1. $b > 1$

In Fig. 2(a) a limit cycle exists on the circle $r = 1$ (denoted by I) as in the case of model 1.

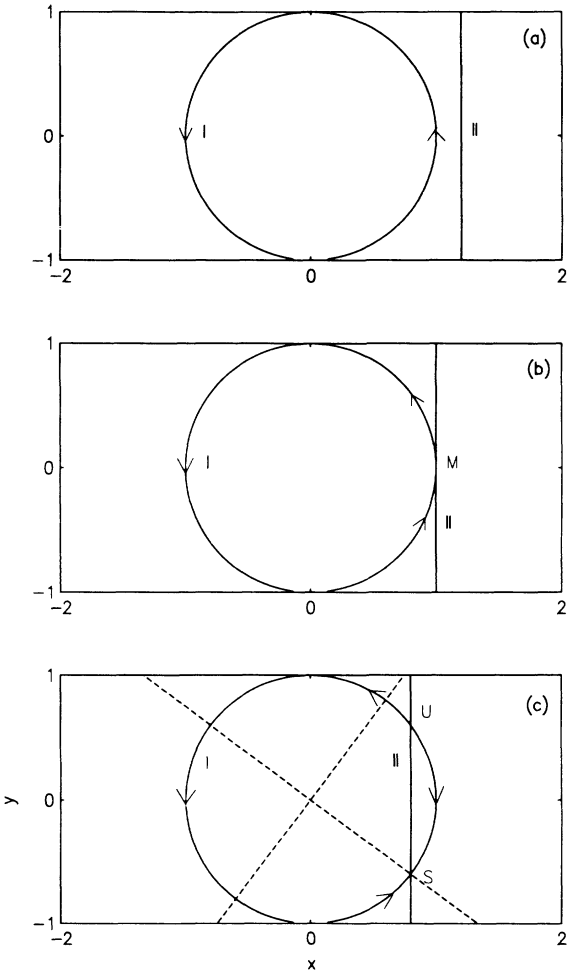

FIG. 2. Deterministic behavior of model 2. (a) $b > 1$, the case of the limit cycle. (b) $b = 1$, one fixed point with marginal stability. A homoclinic orbit exists as indicated by the arrows. (c) $b < 1$, one stable and one unstable fixed point on the circle $r = 1$. The location of the fixed points is again given by the intersections of the circle I ($r = 1$) and the line II, defined by $b = x$.

2. $b=1$

The dynamics is similar to that of model 1 for the same b. The two fixed points and the two heteroclinic orbits of model 1 in Fig. 1(b) are replaced by one fixed point and a homoclinic orbit running anticlockwise in Fig. 2 (b).

3. $b<1$

Instead of the four fixed points for model 1 there are two stationary solutions on the circle $r=1$,

$$r=1, \quad b=\cos\phi \ , \tag{12}$$

one stable and the other unstable, denoted again by S and U in Fig. 2(c), respectively.

The essential difference between the models 1 and 2 is that in the case 3 the former is bistable (or marginally bistable in the case 2) while the latter is monostable (or marginally monostable in the case 2). With model 2 we want to emphasize in the following that bistability is not a necessary ingredient for the SR effect. This agrees with the conclusion in [12], though the mechanism of the SR in our model 2 is essentially different from that of the system in Ref. [12]. The advantage of our two models is that they manifest successively a number of typical distinctive deterministic behaviors, namely, bistability, heteroclinic orbits, and limit cycle solution for model 1, and monostability, homoclinic orbit, and limit cycle for model 2, by changing only a single parameter b.

In the following we will consider the influence of white noise on the above deterministic pictures. By including noise, one can no longer provide an exact solution to either model 1 or model 2. It is necessary to invoke numerical simulation to investigate the behavior of the Langevin equations (1) and (2).

An important quantity we use is the power spectrum which is defined in the following way. For a given set of parameters (b,D) we consider 500 independent time series $[x(k,t),y(k,t)$ for $k=1,\ldots,500]$ obtained from Eqs. (1) and (2) and calculate the corresponding Fourier transformations $[\tilde{x}(k,\omega),\tilde{y}(k,\omega)]$. The spectrum is then defined as

$$\langle S_x(\omega)\rangle=\sum_{k=1}^{500}|\tilde{x}(k,\omega)|^2/500 \ . \tag{13}$$

For y we have the same definition. This is the so-called consensus spectrum. To further describe the quality of the output spectrum quantitatively we define a "quality factor" β of the spectrum of a time series as

$$\beta=\omega_p\frac{h}{W} \ . \tag{14}$$

Thereby h is the maximum peak height of the spectrum and W the width of the spectrum peak defined at the height of $h/\sqrt{e}$. ω_p is the peak frequency of the spectrum. Then β is nothing but the quality factor with its conventional meaning. With finite h and ω_p, we have $\beta\to\infty$ as $W\to 0$, namely, we get a pure signal coming from the inner system dynamics. With noise we certainly have no zero W and reduced β, and the signal becomes ambiguous. Thus, the quantity β may well represent the quality of the signal, i.e., it shows how well we can obtain the coherent oscillation of the system. We then term β the signal-to-noise ratio.

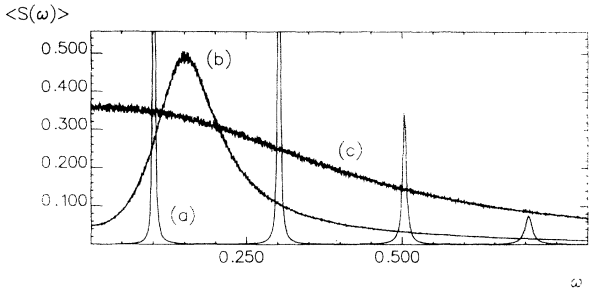

FIG. 3. Spectra of $y(t)$ for $b=1.05$ and $D=3.0\times10^{-5}$ (a), $D=0.05$ (b), and $D=0.9$ (c). (All the figures from Fig. 3 to Fig. 10 are obtained by numerically simulating the Langevin equations of model 1.)

III. STOCHASTIC RESONANCE WITHOUT EXTERNAL PERIODIC FORCE

A. Model 1

1. $b>1$, the case of the deterministic limit cycle

First, let us consider the case of a deterministic limit cycle ($b>1$), and investigate how the coherent motion displayed by the limit cycle is influenced by noise.

Figure 3 shows the spectra of time series of $y(t)$ for $b=1.05$ and for three different values of the noise strength D. The scaling on the ω axis is arbitrary. For a very small noise strength we have very narrow and high spectrum peaks at the frequency of the deterministic limit cycle and its odd-order harmonics [curve (a), $D=3.0\times10^{-5}$]. The absence of even-order harmonics is due to the symmetry of Eqs. (5) and (6), invariant with respect to the reflection $x,y\to-x,-y$. As we increase noise the spectrum becomes wider and lower. At the same time the peak frequency is considerably shifted [curve (b), $D=0.05$]. We emphasize that the profile of Fig. 3(b) is typical for a limit cycle subject to noise. The

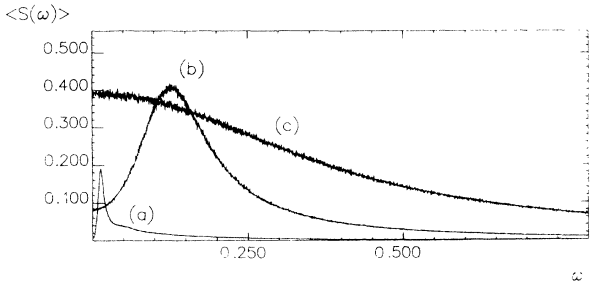

FIG. 4. Spectra of $y(t)$ for the case $b=1$ and $D=3.0\times10^{-5}$ (a), $D=0.05$ (b), and $D=0.9$ (c).

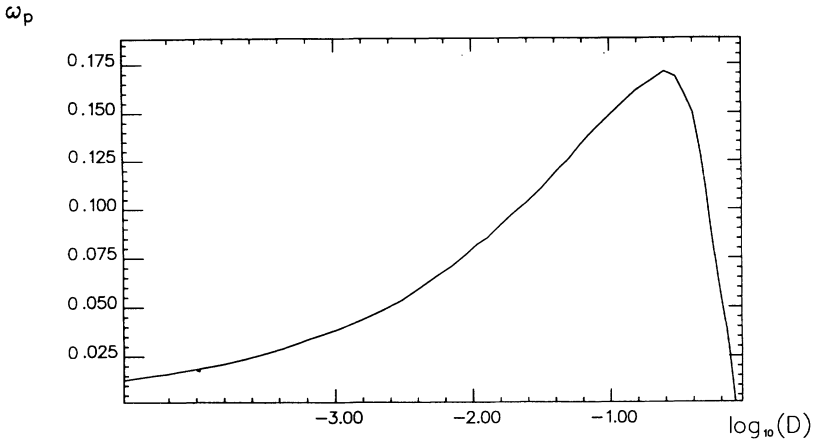

FIG. 5. ω_p plotted against $\log_{10}(D)$ for $b=1$.

peak is centered at a finite frequency. This indicates the existence of a coherent motion (signal of the system dynamics), while the width of the peak shows the influence of the random force. For still larger D [Fig. 3 (c), $D=0.9$] the maximum of the spectrum is shifted to zero frequency. The collective oscillation with a preferred nonzero frequency is thus destroyed by the large noise. The spectrum is of a purely random nature.

Now one point is worth mentioning. Without noise, there is a δ function in the spectrum at the frequency of the limit cycle. The inclusion of noise reduces the δ function to a spectrum peak of finite height. This point is essentially different from the behavior of noise-driven and periodically forced systems. In the latter case, a δ peak certainly remains after adding noise.

2. *b = 1, the case of deterministic heteroclinic orbits*

In this case we have an interaction between two heteroclinic orbits and the noise. Without any noise the system will approach one of the two semistable fixed points. Here the anticlockwise heteroclinic orbits of the deterministic system offer the possibility for anticlockwise rotations. However, without noise the rotation is stopped by the fixed points, and no persistent oscillation can occur. The added noise helps to drive the system away from the fixed points. As a feedback, the resulting small shift along the unstable manifold of each fixed point will be amplified by the deterministic dynamics, leading the system to escape from the fixed points through the unstable directions and to approach the other fixed points through the stable manifolds [see Fig. 1(b)], and a complete circulation of coherent motion on the circle $r=1$ could result, just like the motion in the limit cycle system. Thus, it is very interesting to investigate how the noise-induced coherent motion can be influenced by the noise strength. Since we have the deterministic stationary solutions at $x=\pm 1$, $y=0$, the state $y(t)=0$ can be regarded as the absence of coherent motion, and the oscillation of $y(t)$ may serve as the order parameter to measure the coherence of the system.

Figure 4 shows a set of spectra $\langle S_y(\omega)\rangle$ with respect to

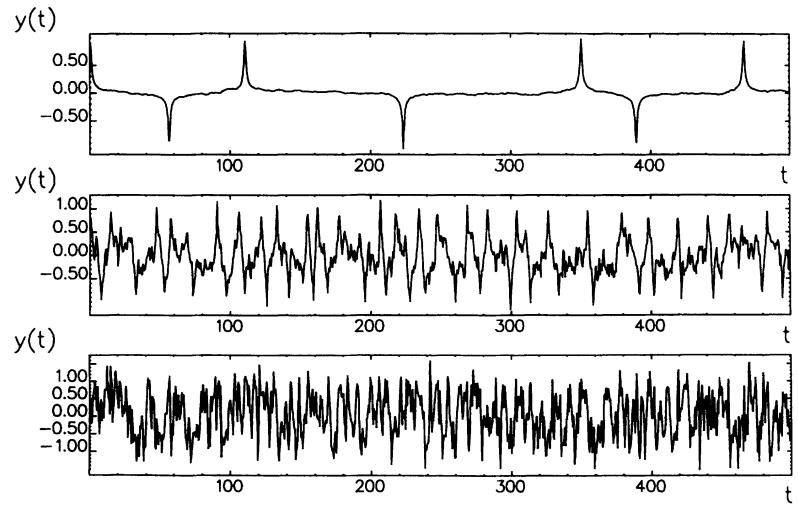

FIG. 6. Time series of $y(t)$ for various D. All the parameters are the same as in Fig. 4.

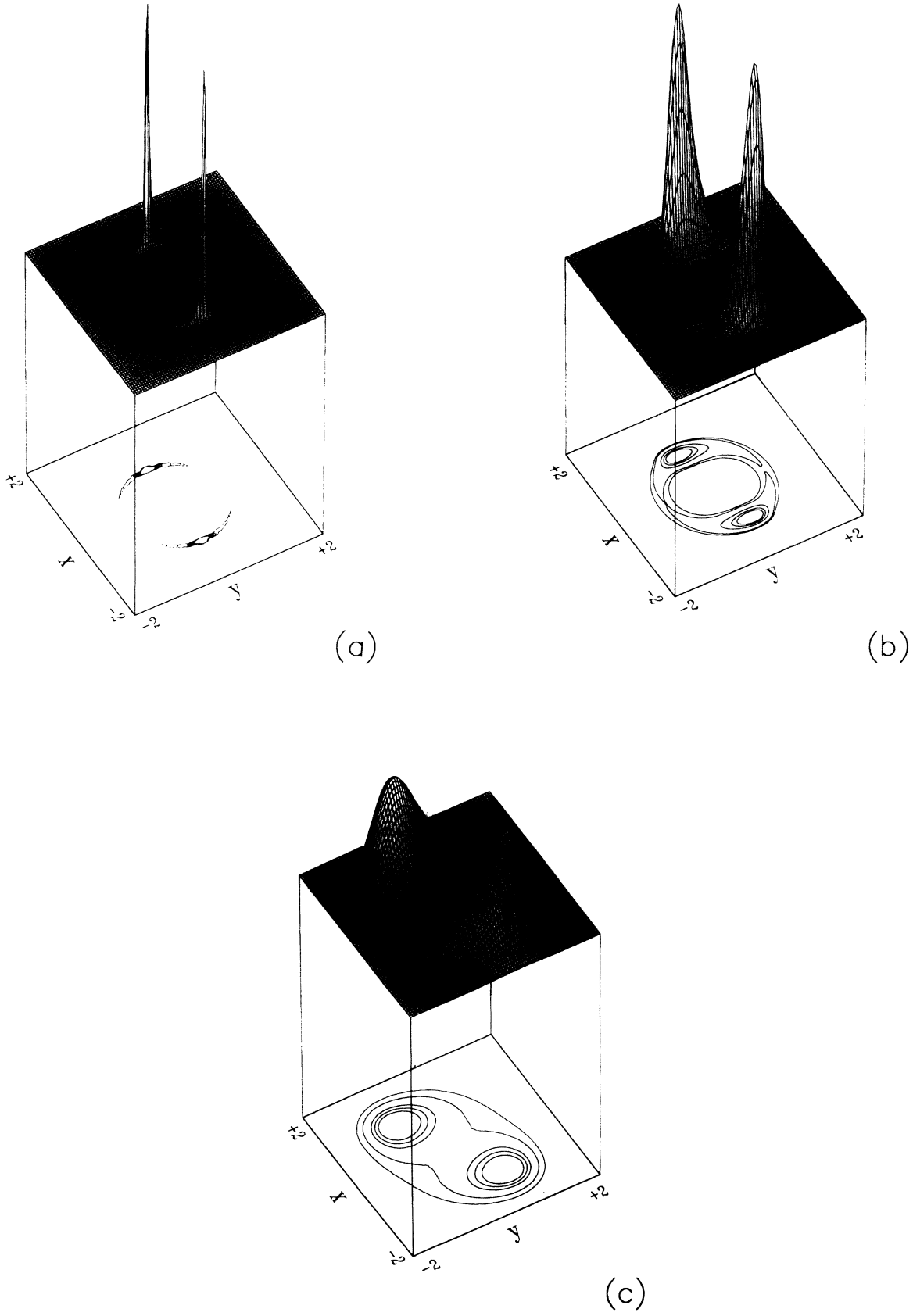

FIG. 7. Probability distributions and the level curves of the distributions plotted in the x-y phase plane for $b=1$. The D values are the same as those in Fig. 4.

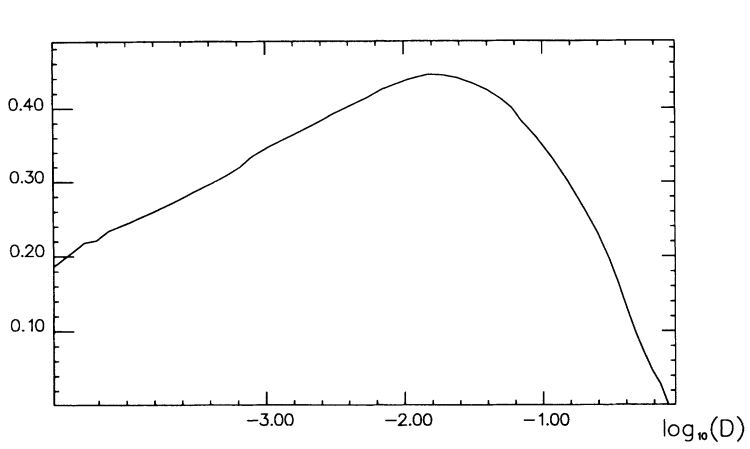

FIG. 8. β is plotted vs $\log_{10}(D)$ for $b=1$. A resonancelike response, i.e., SR, can be clearly seen.

frequency ω for different values of D for the critical parameter $b=1$. For small D we find a small spectrum peak at a very small frequency [Fig. 4(a), $D=3.0\times10^{-5}$]. With the increase of D both the position (ω_p) and the height (h) of this spectrum peak increase [Fig. 4(b), $D=0.05$]. The resemblance of Figs. 4(b) and 3(b) convinces us that there exists indeed a strong coherent motion which is stimulated purely by noise. For a certain large D the peak height h starts to decrease. For slightly larger D, the peak center frequency ω_p decreases, too. Finally, for sufficiently large D the maximum of the spectrum is shifted to the zero frequency [Fig. 4(c)]. Then the dynamics is dominated by a random motion.

In Fig. 5 ω_p is plotted against $\log_{10}(D)$. ω_p increases as D increases for low values of D until a maximum is reached. If we increase D further ω_p decreases again. After a certain critical value D $\omega_p=0$ is reached identically. The disappearance of the preferred finite frequency indicates the complete control over the system by the strong noise.

The behaviors shown in Figs. 4 and 5 can be understood more clearly by looking at Figs. 6 and 7. Figure 6 shows the time series of $y(t)$ for the three different parameter values of D as in Fig. 4. For very small D [Fig. 6(a)] the system can hardly escape from the deterministic fixed points; thus we have $y(t)=0$ for almost all the time. This fact is reflected by the small h and small ω_p in Fig. 4(a). As D increases the system has more and more chances to run along the heteroclinic orbits. Thereby upward and downward pulses in Fig. 6 occur. At a certain value of D the noise-generated pulses form a coherent oscillation with its frequency fluctuating around a finite value ω_p. At the same the noise level is still quite low [see Fig. 6(b)]. This particular noise strength, which seems to be an optimum for the noise-induced oscillation, will be analyzed later on. For very large D [e.g., Fig. 6(c)], the time series consists of completely random data, from which one can hardly see any trace of coherent motion. This agrees with the spectrum Fig. 4(c).

In Fig. 7 we plot the probability distributions of the system in the x-y phase space and the corresponding level curves, for the same D values as in Fig. 4. These figures show three kinds of typical distinctive behavior again. In Fig. 7(a) the probability concentrates, for very small D, at the fixed points and the coherent oscillation is extremely weak. In Fig. 7(b), at the optimum D, a considerable amount of probability distributes along the circle $r=1$ which leads to a limit-cycle-like motion. As the noise increases further, the distribution hump on the circle $r=1$ becomes wider. For sufficiently large noise, as in Fig. 7(c), the probability distribution has a topological change. The circle hump disappears and a saddle point of the distribution appears at the origin. In this case the probability exchanges between the two basins mainly occur through the center saddle point rather than the circle, and a rotation with a characteristic frequency can no longer be observed. This explains the destruction of the coherent oscillation in Figs. 3(c) and 4 with $\omega_p\to0$ for large D.

Figures 4–7 imply the existence of an optimum noise strength which produces the "best" oscillation. Either too small or too large noise will definitely destroy the coherent motion of the system. This fact and the overall response of the system to the noise can be well represented and quantitatively measured by the quality factor (or the SNR) β. In Fig. 8 β is plotted versus $\log_{10}(D)$. We see an unambiguous maximum of β at a certain D. This maximum clearly confirms the existence of the optimum

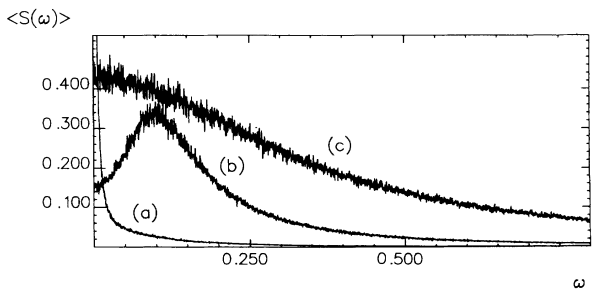

FIG. 9. Spectra of $y'(t)$ for $b=0.95$ and for $D=0.004$ (a), $D=0.05$ (b), and $D=0.9$ (c).

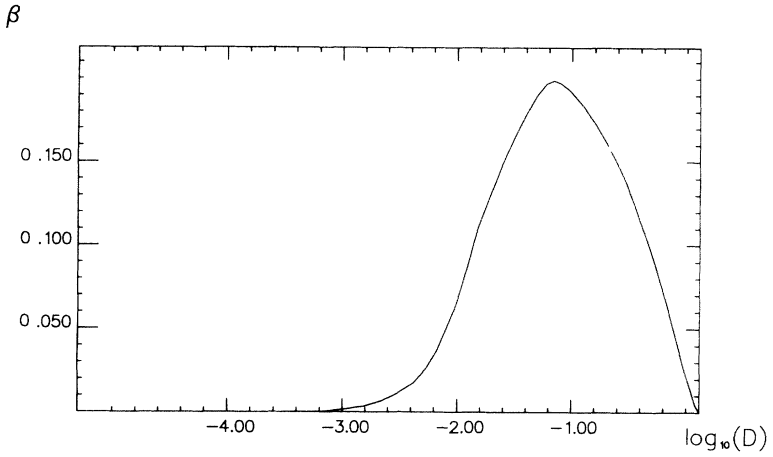

FIG. 10. β against $\log_{10}(D)$ for $b=0.95$. One can see the SR effect below the saddle-node bifurcation threshold.

response of the system to the noise added. This behavior very much resembles the usual SR phenomenon. Thus, we call this optimum response "SR without periodic force."

However, there is an incompleteness in this analogy. In the usual SR case, there is a predefined frequency of the periodic signal. The peak of the power spectrum for the output is not shifted if one changes the noise strength. In our system there is no such predefined external signal and the preferred periodicity is induced by noise. The peak frequency can be considerably shifted by the noise strength. The noise-induced coherent oscillation and frequency shift have been well investigated in the past (e.g., [15] and references therein). Here our emphasis focuses on the existence of the optimal noise strength for such a noise-induced oscillation.

3. $b < 1$, bistable stationary solutions

Without noise the system will asymptotically approach one of the two stable points, depending on the initial condition. By rotating the coordinates according to

$$x' = x\cos\phi_0 + y\sin\phi_0 \tag{15}$$

$$y' = -x\sin\phi_0 + y\cos\phi_0, \quad \phi_0 = -\tfrac{1}{2}\arccos(b)\ , \tag{16}$$

we set the stable points on the x' axis, namely, at $x'=\pm 1$, $y'=0$. The x' and y' axes are denoted by dotted lines in Fig. 1. Now we can take y' as order parameter. We asymptotically have $y'(t)=0$, corresponding to no coherent motion in the deterministic system. Any coherent motion or any oscillation of nonzero $y'(t)$ should be stimulated by adding noise. Figure 9 shows the spectra with respect to frequency for $b=0.95$ and various D values. For very small D, we only find a nearly straight line spectrum at $\omega=0$ [Fig. 9(a)], indicating that the system is attracted to the close vicinity of one of the fixed points. With the increase of D the spectrum is deformed to a peak with the center ω_p located at a small nonzero frequency, showing the presence of occasional switchings between two basins. Both the center frequency ω_p and the height h of the peak increase with increasing D in the first stage [see Fig. 9(b)]. For a certain value of D, h starts to decrease, and then ω_p decreases subsequently, too. Finally, for sufficiently large D the center frequency moves to zero; then the coherent oscillation stimulated by the noise is destroyed by the noise itself almost completely. In Fig. 10 β is plotted against D for $b=0.95$. A resonance peak is also apparent. Hence the SR without external periodic force can be observed as well below the saddle-node bifurcation threshold.

Comparing Figs. 9, 10 with 4, 8 it is clear that, when the parameter is below the critical value ($b<1$), the SR effect is less effective than that for the critical parameter $b=1$. We also considered the case of even smaller b's. The general tendency is that the smaller b is (the deeper the system sinks to the attracting basin of stable points), the more difficult it is for the system to have an optimum response. This effect can be interpreted as follows. The barrier between the stable and the unstable points which the system has to overcome with the help of noise increases with the decrease of b. Then we can easily imagine that for sufficiently small b the required D value for the system to overcome the barrier becomes so large that any coherent oscillation of the system, which might be

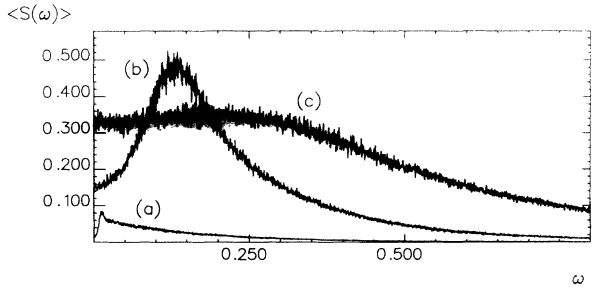

FIG. 11. Spectra of $y(t)$ in model 2 for $b=1$ and $D=3.0\times10^{-5}$ (a), $D=0.05$ (b), and $D=0.9$ (c). (All the figures from Fig. 11 to Fig. 13 are obtained by numerically simulating the Langevin equations of model 2.)

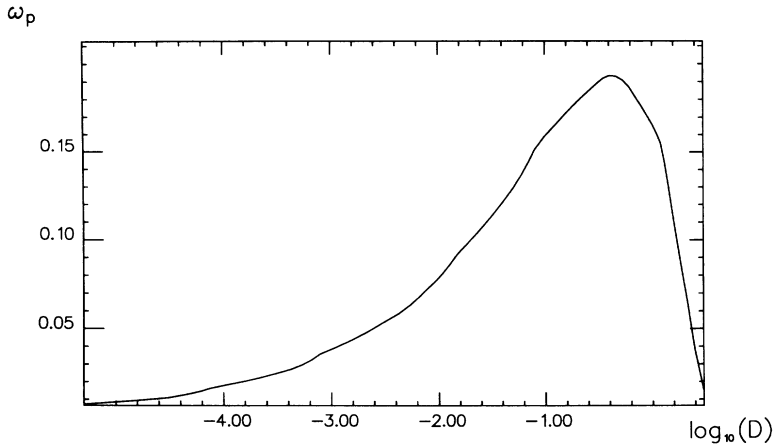

FIG. 12. ω_p plotted against D for $b=1$.

activated by noise, could be well destroyed by such a large noise. As a result there is no optimum response of the system for sufficiently small b.

B. Model 2

In model 1 we have two asymptotic stationary solutions for $b \leq 1$, i.e., we are dealing with the case of bistability. The problem arises whether bistability is a necessary condition for SR in autonomous systems. We try to deal with this problem by investigating model 2. The following numerical results give a definite negative answer to this question.

We focus on the parameter value $b=1$, i.e., on the critical condition. In Fig. 11 the spectra are plotted against ω for various D. The behavior is rather similar to that in Fig. 4. For very small D [Fig. 11(a), $D=3.0\times10^{-5}$], we find a very low peak with a very small center frequency. Corresponding to that the system spends a major portion of time in the vicinity of the fixed point $x=1$, $y=0$. There are very seldom such events that the system is driven by small noise away from the fixed point along the unstable manifold. Then it is driven by the deterministic force to travel along the homoclinic circle. As D increases, the events of the circulation along the loop $r=1$ happen more and more frequently. Consequently we get a stronger and stronger coherent oscillation. However, the situation is essentially changed for sufficiently large D. After a certain D [Fig. 11(b), $=0.05$] the peak height and the peak frequency start to decrease on further increasing D. In Fig. 11(c), at $D=0.9$, the spectrum peak approaches zero. This indicates the domination of noise over the motion of the system.

In Fig. 12 the peak frequency ω_p is plotted against $\log_{10}(D)$. The behavior is again similar to that of Fig. 5. For sufficiently large D, ω_p approaches zero.

The SR phenomenon can be seen in Fig. 13, where the β-D curve is plotted for model 2. We have therefore identified the existence of SR for monostable autonomous systems. All the figures from Fig. 11 to Fig. 13 for the monostable system are similar to those from Fig. 4 to Fig. 8 for the bistable systems, apart from one difference: The two deterministic fixed points and two heteroclinic orbits seen in Fig. 6 and 7 are replaced by one deterministic fixed point and a single homoclinic orbit. We have also examined the cases of $b>1$ and $b<1$ for model 2. The general features are similar to those in Figs. 3, 9, and 10. We will not present them further here.

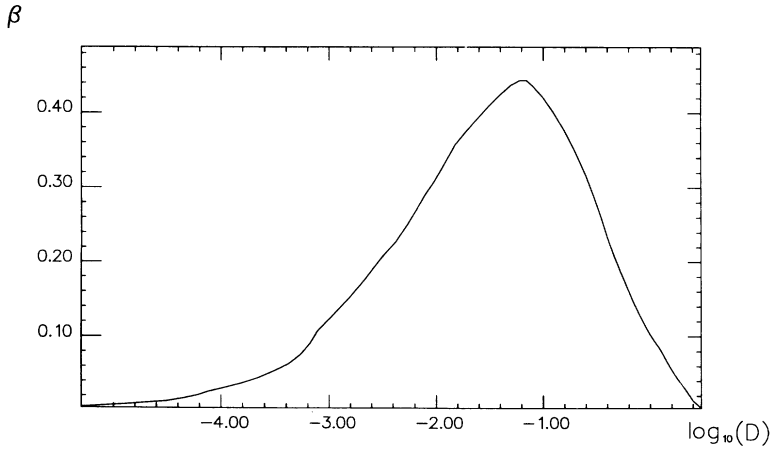

FIG. 13. β against $\log_{10}(D)$ for $b=1$. The SR effect can be observed equally as well in the monostable system as in the bistable system (Fig. 8).

IV. CONCLUDING REMARKS

To conclude this paper we would like to make the following remarks.

First, some noise-induced oscillations have been observed in various systems due to different mechanisms and have been reported in a number of papers [15–17]. Here we consider more general two-dimensional autonomous systems. As $b \leq 1$ the asymptotic states of both models 1 and 2 are steady solutions which do not display any coherent oscillation. Nevertheless, coherent rotations do exist in the transient processes when the systems are away from the fixed points. Precisely speaking, the deterministic systems intrinsically include a symmetry breaking in favor of the anticlockwise rotations in both models even for $b \leq 1$. However, these coherent oscillations cannot be observed in the asymptotic states due to the attracting property of the fixed points. In this case noise may play an active role in inducing coherent oscillation. In particular, the response of the autonomous system to the noise can show a resonancelike behavior, the SR without external periodic force.

Second, the reason for the SR peaks in Figs. 8, 10, and 13 is physically clear. In these models noise plays a twofold role. On the one hand, it activates coherent motion by driving the systems away from the asymptotic fixed points and by transferring the transient circulations of the deterministic systems to asymptotic collective oscillations. On the other hand, the noise naturally spoils the coherent motion stimulated by itself. In the positive slope regions of Figs. 8, 10, and 13 the former tendency dominates and we have monotonically increasing β-$\log_{10}(D)$ curves. In the regions of negative slope, the latter tendency dominates and the curves go down.

Third, we realize that bistability is not a necessary ingredient for the SR in our autonomous systems. This conclusion agrees with that in Ref. [12]. Our model 2 has only a single asymptotic steady solution for $b \leq 1$, in which the SR effect can be observed equally well as in the bistability case. Nevertheless, the mechanism of SR in our monostable system is essentially different from that in Ref. [12]. In the latter case, the optimum noise plays a role in driving the system to the deterministic trajectories which have frequencies close to the frequency of the external periodic force. Then the input force can be amplified by the resonance. Driven by smaller or larger noises, the system may have more probability to stay in the trajectories far away from the deterministic resonance condition with the external force, and then the output signal amplitude is much smaller. Therefore the SR in Ref. [12] is very similar to the deterministic resonance in mechanics and other fields, as the authors correctly concluded. In our model 2, no external frequency exists. The SR-like behavior is due to a mechanism exactly the same as that for bistable systems, i.e., the competition of the twofold roles played by noise, stimulating coherent motion on one hand and spoiling the coherent oscillation stimulated by itself on the other hand. Then the SR in our monostable system has a meaning similar to the conventional meaning of SR.

Finally, the same behavior as in our model can be easily found in many systems displaying self-organization structures [18], for example, in biology or psychology [19]. Therefore the effects revealed in this paper are expected to have wide applications in various nonlinear systems subject to stochastic forces.

ACKNOWLEDGMENTS

We wish to thank Professor H. Haken for his continuous support and for critical reading of the manuscript. C. Z. Ning acknowledges the support of the Deutsche Forschungsgemeinschaft (DFG) through SFB 329. G. H. thanks the University of Stuttgart for financial support of his visit.

[1] R. Benzi, A. Sutera, and A. Vulpiani, J. Phys. A **14**, 453 (1981); R. Benzi, G. Parisi, A. Sutera, and A. Vulpiani, Tellus **34**, 10 (1982).

[2] C. Nicolis and G. Nicolis, Tellus **33**, 225 (1981); C. Nicolis, *ibid.* **34**, 1 (1982).

[3] B. McNamara and K. Wiesenfeld, Phys. Rev. A **39**, 4853 (1989).

[4] R. Fox, Phys. Rev. A **39**, 4148 (1989).

[5] T. Zhou and F. Moss, Phys. Rev. A **41**, 4255 (1990).

[6] L. Gammaitoni, F. Marchesoni, E. Menichella-Saetta, and S. Santucci, Phys. Rev. Lett. **62**, 349 (1989).

[7] G. Hu, G. Nicolis, and C. Nicolis, Phys. Rev. A **42**, 2030 (1990).

[8] A. Longtin, A. Bulsara, and F. Moss, Phys. Rev. Lett. **67**, 656 (1991).

[9] P. Jung and P. Hänggi, Europhys. Lett. **8**, 505 (1989); Phys. Rev. A **44**, 8032 (1991).

[10] M. I. Dykman, R. Mannella, P. V. E. McClintock, and N. G. Stocks, Phys. Rev. Lett. **68**, 2985.

[11] G. Hu, H. Haken, and C. Z. Ning, Phys. Rev. E **47**, 2321 (1993).

[12] N. G. Stocks, N. D. Stein, and P. V. E. McClintock, J. Phys. A **26**, L385 (1993).

[13] G. Hu, T. Ditzinger, C. Z. Ning, and H. Haken, Phys. Rev. Lett. **71**, 807 (1993).

[14] G. Hu and B. L. Hao, Phys. Rev. A **42**, 3456 (1990).

[15] H. Risken, *The Fokker-Planck Equation* (Springer, Berlin, 1984).

[16] L. Fronzoni, R. Mannella, P. V. E. McClintock, and F. Moss, Phys. Rev. A **36**, 834 (1987).

[17] A. Irwin, S. Fraser, and R. Kapral, Phys. Rev. Lett. **64**, 2343 (1990); B. Caveau, E. Gudovska-Nowak, R. Kapral, and M. Moreau, Phys. Rev. A **46**, 825 (1992).

[18] H. Haken, *Advanced Synergetics* (Springer, New York, 1983).

[19] T. Ditzinger and H. Haken, Biol. Cybern. **61**, 279 (1989); **63**, 453 (1990).

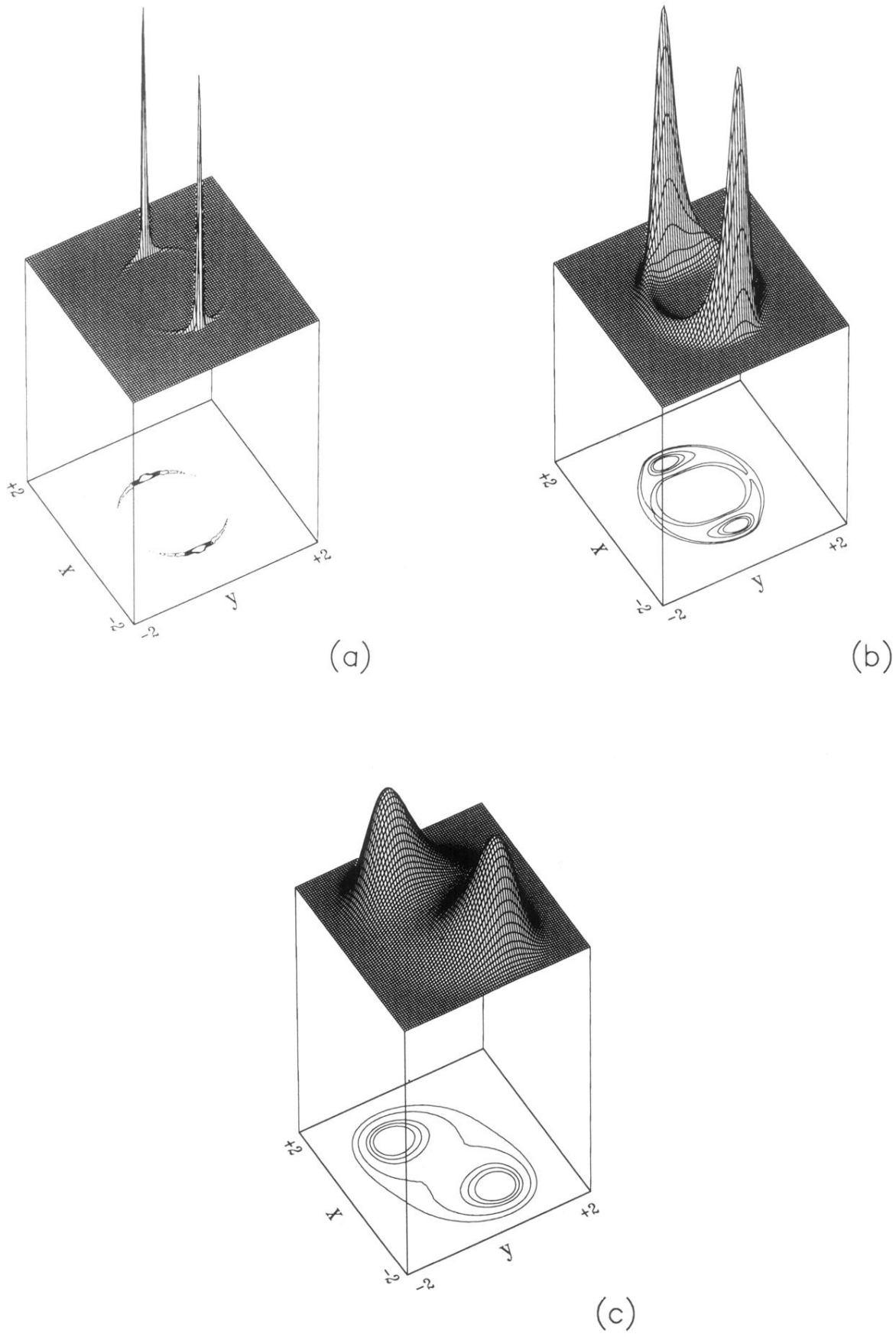

FIG. 7. Probability distributions and the level curves of the distributions plotted in the x-y phase plane for $b=1$. The D values are the same as those in Fig. 4.